



Trifluoperazine Synergistically Potentiates Bortezomib-Induced Anti-Cancer Effect in Multiple Myeloma via Inhibiting P38 MAPK/NUPR1

Zizi Jing,¹ Wei Yu,¹ Anmao Li,² Xuanxin Chen,¹ Yuying Chen¹ and Jianbin Chen¹

¹Department of Hematology, The First Affiliated Hospital of Chongqing Medical University, Chongqing, China

²Department of Respiratory, The First Affiliated Hospital of Chongqing Medical University, Chongqing, China

Multiple myeloma (MM) is a common hematological malignancy. Bortezomib (BTZ) is a traditional medicine for MM treatment, but there are limitations for current treatment methods. Trifluoperazine (TFP) is a clinical drug for acute and chronic psychosis therapy. Lately, researchers have found that TFP can suppress tumor growth in many cancers. We attempted to study the effects of BTZ and TFP on MM *in vivo* and *in vitro*. We concentrated on the individual and combined impact of BTZ and TFP on the proliferation and apoptosis of MM cells via Cell Counting kit-8 assay, EdU assay, western blot, and flow cytometry. We found that combination therapy has a strong synergistic impact on MM cells. Combination therapy could induce cell arrest during G2/M phase and induce apoptosis in MM cells. Meanwhile, BTZ combined with TFP could play a better role in the anti-MM effect *in vivo* through MM.1s xenograft tumor models. Furthermore, we explored the mechanism of TFP-induced apoptosis in MM, and we noticed that TFP might induce MM apoptosis by inhibiting p-P38 MAPK/NUPR1. In summary, our findings suggest that TFP could synergistically enhance the BTZ-induced anti-cancer effect in multiple myeloma, which might be a promising therapeutic strategy for MM treatment.

Keywords: apoptosis; bortezomib; cell cycle; multiple myeloma; trifluoperazine

Tohoku J. Exp. Med., 2022 August, 257 (4), 315-326.

doi: 10.1620/tjem.2022.J044

Introduction

Multiple myeloma (MM) is one of the malignant plasma cell diseases in which tumor cells are derived from bone marrow plasma cells (Mateos and San Miguel 2017). With the development of medical technology, the diagnostic rate of multiple myeloma is increasing. The incidence of MM is about 2~3/100,000, and the female to male ratio is 1:1.6; most patients are over 40 years old. Since the proteasome inhibitor was approved for MM treatment, Bortezomib (BTZ) has dramatically alleviated the patient's condition. However, multiple myeloma is still incurable (Turner et al. 2013). After using BTZ, the possible side effects of patients include gastrointestinal symptoms, thrombocytopenia, weakness (fatigue, malaise, and weakness), and peripheral neuropathy (Argyriou et al. 2008; San Miguel et al. 2008; Richardson et al. 2010; Kumar et al. 2012). More, unfortunately, many patients develop primary

or secondary drug resistance after BTZ treatment (Robak et al. 2018). Therefore, there is an urgent need to find a useful drug to overcome the BTZ chemoresistance and ameliorate the clinical outcomes of MM. Researchers have used combined strategies in cancer chemotherapy for a long time to improve efficacy and reduce side effects (Ackler et al. 2010; Galmarini et al. 2012; Palumbo and Cavallo 2012).

Trifluoperazine (TFP) is an anti-psychotic drug to treat acute and chronic psychosis (Huang et al. 2019). Recently, researchers have discovered that TFP has anti-tumor effects on breast cancer, glioblastoma, and colorectal cancers (Kang et al. 2017; Feng et al. 2018; Qian et al. 2019). Our previous study suggested that TFP could induce apoptosis in U266 and RPMI 8226 cells by targeting NUPR1 *in vitro* (Li et al. 2020).

A study reported that the proteasome inhibitors enhanced the accumulation of misfolded and unfolded proteins, improved the efficacy of TFP against pancreatic can-

Received March 8, 2022; revised and accepted May 17, 2022; J-STAGE Advance online publication May 27, 2022

Correspondence: Jianbin Chen, Department of Hematology, The First Affiliated Hospital of Chongqing Medical University, No 1 YouYi Road, Yuzhong, Chongqing 400016, People's Republic of China.

e-mail: cqchejianbin2007@126.com

©2022 Tohoku University Medical Press. This is an open-access article distributed under the terms of the Creative Commons Attribution-NonCommercial-NoDerivatives 4.0 International License (CC-BY-NC-ND 4.0). Anyone may download, reuse, copy, reprint, or distribute the article without modifications or adaptations for non-profit purposes if they cite the original authors and source properly.

<https://creativecommons.org/licenses/by-nc-nd/4.0/>

cer (Huang et al. 2019). Here, we investigate the effects of TFP combined with BTZ *in vivo* and *in vitro* to explore whether TFP could promote proteasome-based chemotherapy in multiple myeloma, attempting to provide a new approach for MM treatment.

Methods

Cell culture

The multiple myeloma cells, U266 and MM.1S, were obtained from the Beijing Cell Bank of the Chinese Academy of Sciences (Beijing, China) and the Shanghai Cell Bank of the Chinese Academy of Sciences (Shanghai, China), respectively. Cells were grown in a complete medium consisting of 90% RPMI1640 (Sigma, St. Louis, MO, USA), 10% fetal bovine serum (PAN-Biotech Ltd., Aidenbach, Germany), 100 µg/ml streptomycin, and 100 U/ml penicillin composition at 37°C in a humidified incubator with 5% CO₂. Bortezomib (purity = 98.95%) and Trifluoperazine dihydrochloride (purity > 99.0%) were purchased from MedChemExpress (Monmouth Junction, NJ, USA).

CCK-8 assay and combination index determination

Cell Counting Kit-8 (CCK-8) assay was employed to assess cell viability. MM cells were resuspended, adjusted the cell density to 5×10^4 cells/ml, and transferred 100 µl cell suspension into a 96-well plate; various concentrations of BTZ and TFP were employed in U266 and MM.1S for 48 h, respectively. Then, the CCK-8 reagent (Bimake, Houston, TX, USA) was incubated with MM cells in the dark for 2 h. Finally, a microplate reader (Thermo Fisher Scientific, Waltham, MA, USA) measured OD values at 450 nm. SPSS software (IBM, version 26.0) was used to calculate half-maximal inhibitory concentration (IC₅₀). According to the Chou-Talalay method, MM cells were treated with BTZ combined with TFP at a fixed ratio for 48 h. The CompuSyn software was used to calculate the combination index (CI), which indicates interaction between drugs. CI > 1.10 represents antagonism; CI < 0.90 represents synergism, and CI between 0.90 and 1.10 represent additive effects.

EdU proliferation assay

MM cells were pretreated with EdU work solution (Beyotime, Nanjing, China) for 3 h, then collected and fixed with methanol and acetic acid for 30 min, and penetrated with 0.3% Triton X-100 for 15 min at room temperature. Next, cells were washed with phosphate-buffered saline (PBS) three times and cultured with 0.1 ml of the click reaction mixture for 30 min at room temperature in the dark. Finally, the cell nucleus was stained with 4',6-diamidino-2-phenylindole (DAPI) for 10 min. The fluorescence microscope (Olympus, Tokyo, Japan) was used to observe and photograph the stained cells.

Cell cycle analysis

MM cells were gathered, washed with pre-cooled PBS, and fixed with 70% cold ethanol overnight at 4°C. Next, cells were washed once with PBS and incubated with 0.2% Triton X-100, propidium iodide (PI) (Sigma), and RNase A at 4°C in the dark for 30 min. Then, cells were analyzed via a flow cytometer (Becton Dickinson, Shanghai, China).

Apoptosis analysis

MM cells were collected and washed with pre-cooled PBS. The apoptotic cells were double-stained with Annexin V-APC/PI (Elabscience, Wuhan, China) based on the manufacturer's instructions. Then, flow cytometer (Becton Dickinson) detects the cell apoptosis rate.

Western blot

Protein extraction reagent RIPA (Beyotime) was applied to extract and purify the proteins from multiple myeloma cells and tumor tissues. The BCA Protein Assay Kit (Beyotime) was applied to measure the concentration of proteins. The protein was segregated by SDS-PAGE gel and transferred onto the PVDF membrane; 5% skimmed milk blocked the membrane for 2 h. Then, the membrane was incubated at 4°C with primary antibodies for at least 8 h as follows: Bcl-2 (1:1,000, #AF6139, Affinity Biosciences, Cincinnati, OH, USA), Bax (1:1,000, #AF0083, Affinity Biosciences), Cleaved Caspase-3 (1:1,000, #AF7022, Affinity Biosciences), Cleaved Caspase-9 (1:1,000, #AF5240, Affinity Biosciences), P38 MAPK (1:750, #WL00764, Wanlei, Shenyang, China), p-P38 MAPK (1:750, #WLP1576, Wanlei), NUPR1 (1:500, #NBP1-98280, Novus, Centennial, CO, USA), GAPDH (1:3,000, #AF7021, Affinity Biosciences), and beta-Actin (1:1,000, #AF7018, Affinity Biosciences). After that, we used horseradish peroxidase (HRP)-labeled goat anti-rabbit IgG (1:1,000, #A0208, Beyotime) to detect the primary antibody. The bands were visualized using an enhanced chemiluminescent kit (Vazyme, Nanjing, China), pictured, and analyzed using Fusion software (Vilber Lourmat, Marne-la-Vallée, France).

In vivo tumor growth model

The animal experiments were conducted in strict accordance with the recommendations in the National Institutes of Health (NIH) Laboratory Animal Care and Use Guidelines. The Animal Experiment Ethics Committee of Chongqing Medical University approved this protocol (No: 2021-529). Approximately 1×10^7 MM.1S cells were injected subcutaneously into five-week-old BALB/c nude mice. When the average tumor volume exceeded 100 mm³, mice were randomly divided into 4 groups: the control, BTZ, TFP, and the combination group (BTZ and TFP). The BTZ group was intravenously injected with BTZ on days 1, 4, 8, and 11 at 0.25 mg/kg. The TFP group was intravenously injected with TFP every two days at 5.0 mg/kg. The administration method and time of the combination group

are the same as those of the single-agent group. The control group was intravenously injected with normal saline only on days 1, 3, 4, 5, 7, 8, 9, 11, 13. The dose of drugs used *in vivo* were determined by the references (Chen et al. 2017; Chen et al. 2018). Bodyweight and tumor volume were recorded every two days. After the administration, all mice were sacrificed, part of tumor tissues and major organs were harvested and fixed with 4% paraformaldehyde, and rest of the tumor tissues were stocked at -80°C .

Immunohistochemistry

Tumor tissues were fixed with 4% paraformaldehyde, embedded with paraffin, and cut into $3\text{-}\mu\text{m}$ -thick tumor tissue sections. The tissue section was deparaffined with xylene; the antigens were repaired with sodium citrate buffer, then hydrogen peroxide blocked the endogenous peroxidase activity. Next, the section was incubated at 4°C with primary antibodies for at least 16 h as follows: Ki-67 (1:200, #12202, Cell Signaling Technology, Danvers, MA, USA), Bcl-2 (1:100, #AF6139, Affinity Biosciences), Bax (1:100, #AF0083, Affinity Biosciences), P53 (1:100, #AF0879, Affinity Biosciences), and Cleaved Caspase-3 (1:100, #AF7022, Affinity Biosciences); then incubated with the secondary antibody for 15 min. After that, the tumor section was stained with 3,3'-diaminobenzidine tetrahydrochloride (DAB) (ZSGB-BIO, Beijing, China).

Hematoxylin-eosin staining

Main organs were harvested and cut into $3\text{-}\mu\text{m}$ -thick sections according to the mentioned method; then we used hematoxylin and eosin to stain the sections according to the instructions. The microscope (Olympus) was used to observe.

Statistical analysis

All experiments were repeated at least three times separately, and data were represented as the mean \pm standard error (SEM). One-way ANOVA and Student's t-test were applied to analyze component differences via GraphPad Prism 8.0. Statistical significance was determined at $*p < 0.05$, $**p < 0.01$, $***p < 0.001$ and $****p < 0.0001$.

Results

TFP synergized the growth inhibitory activity of BTZ on MM cells

We used different concentrations of BTZ and TFP to treat MM cells for 48 h, then CCK-8 assay was used to measure the inhibition rate (Fig. 1A). SPSS software was used to calculate the IC₅₀s. We found that the IC₅₀s of BTZ was 25.383 nM and 14.793 nM in U266 and MM.1S, respectively, and the IC₅₀s of TFP was 25.014 μM and 19.749 μM in U266 and MM.1S, respectively. According to the recommendation of the CI method, we conducted a combined study on U266 and MM.1S at a fixed concentration of 1:1,333 (BTZ: TFP) and 1:1,000 (BTZ: TFP) for 48 h separately. After that, the CompuSyn software was used

to calculate the combination index (CI) (Fig. 1B, C); when we used 25 nM BTZ combined with 25 μM TFP to treat U266 for 48 h, the CI was 0.65, and it indicated that the combination therapy has a synergistic effect (Table 1); when we used 15 nM BTZ combined with 20 μM TFP to treat MM.1S for 48 h, the CI was 0.70, and it indicated that the combination therapy has a synergistic effect (Table 2). Subsequent experiments were investigated using the combined concentrations mentioned above. According to the EdU proliferation assay (Fig. 1D, E), we found that the experimental group significantly reduced cell proliferation compared with the control group. Then, we used CCK-8 to detect the cell viability after MM cells were treated with BTZ, TFP, or BTZ combined with TFP (Fig. 1F). The results revealed that TFP could enhance the cell viability inhibition of BTZ in MM cells.

TFP enhanced the G2/M cell cycle arrest of MM cells induced by BTZ

We used flow cytometry to detect the distribution of cell cycle after MM cells were treated with BTZ or TFP (Fig. 2A). Cells in the experimental groups were arrested in the G2/M phase compared to the control group in MM.1S, and the combination group was significantly higher than the BTZ group. Interestingly, as for U266 cells, there was no significant difference between the TFP and control group, but the combination group was strongly arrested in the G2/M phase compared to the BTZ group ($p = 0.0062$). All those results suggested that TFP might promote the BTZ induced G2/M arrest.

TFP improved the apoptosis-inducing effect of BTZ in MM cells

After cells were treated, we used flow cytometry to detect the apoptosis (Fig. 2B); the apoptosis rate of all the experimental groups was more than the control group, which indicated that both TFP and BTZ could induce apoptosis. In addition, we found that the apoptosis rate in the combination group was more than in the BTZ group ($p < 0.05$). Then we detected the apoptosis-related proteins in MM cells via western blot (Fig. 2C). We noticed that the expression of Bax, Cleaved-Caspase 3, and Cleaved-Caspase 9 was increased, and the expression of Bcl-2 was decreased. The changes in the combination group were more significant than in the BTZ group. These results indicated that TFP could improve the apoptosis-inducing effect of BTZ in MM cells.

TFP combined with BTZ exerted an anti-MM effect in vivo

To verify whether TFP combined with BTZ could play a better role *in vivo*, we constructed the MM.1S xenograft tumor models and randomly divided them into four groups. We recorded the changes in weight and tumor volume (Fig. 3A, B). After the administration, we sacrificed all mice and removed the tumors (Fig. 3C), and recorded the weight of tumors (Fig. 3D). We found that the tumor volume had a

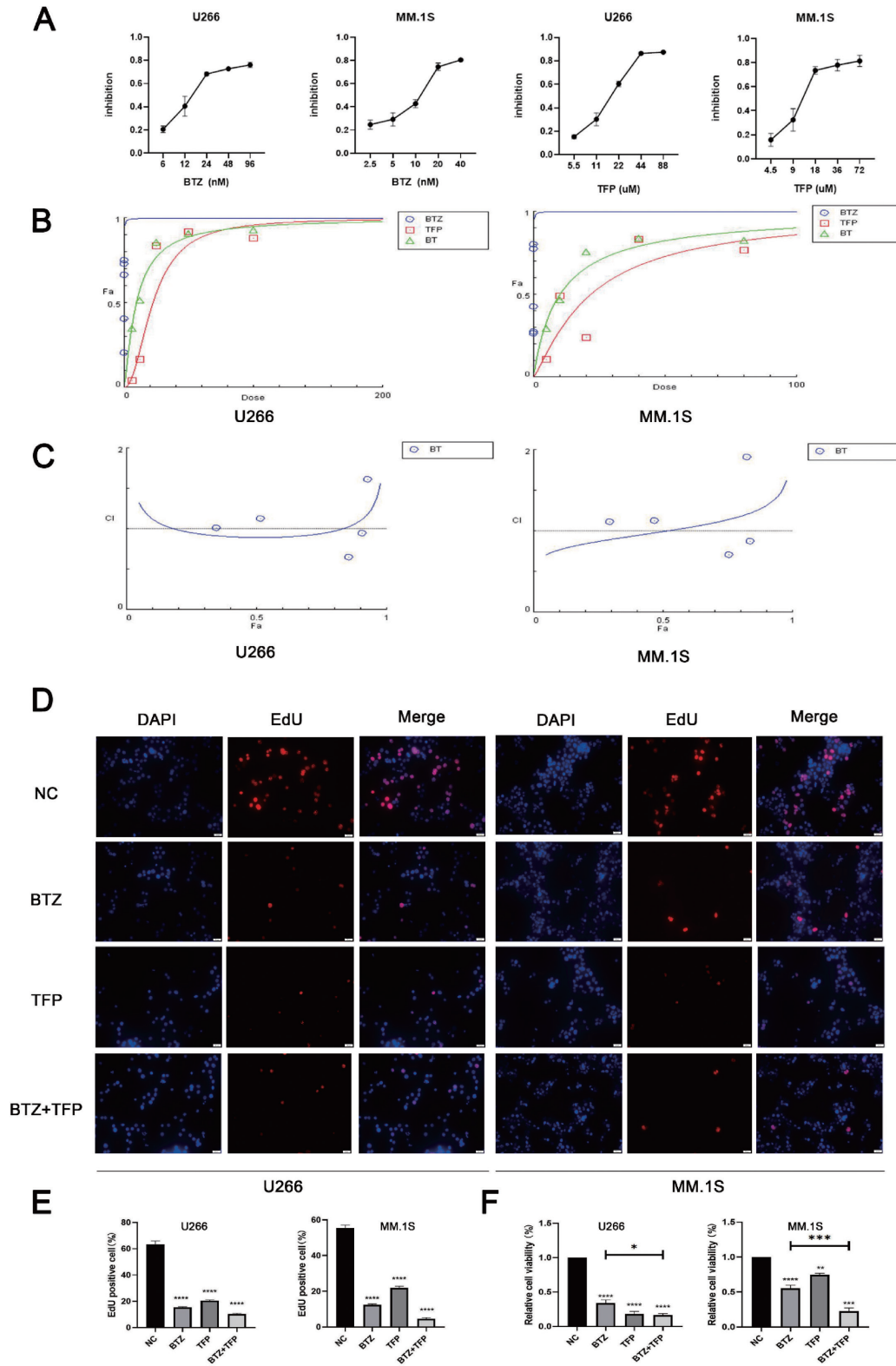


Fig. 1. Trifluoperazine (TFP) synergized the growth inhibitory activity of Bortezomib (BTZ) on multiple myeloma cells. CCK-8 was used to detect the cell viability after treatment with BTZ or TFP in MM cells (A). CompuSyn software was used to calculate the combination index (CI) after treating with BTZ and TFP alone or combination. Dose-effect curves (B) and CI plot (C) are shown. EdU assay was used to detect the proliferation after MM cells were treated with BTZ, TFP, or BTZ combined with TFP (D). Statistical analysis of EdU positive cells (E). CCK-8 assay was used to detect the cell viability after MM cells were treated with BTZ, TFP, or BTZ combined with TFP (F). Data are shown as mean \pm SEM for three replicate determinations. * $p < 0.05$, ** $p < 0.01$, *** $p < 0.001$, **** $p < 0.0001$. BT means BTZ+TFP.

Table 1. Assessment of combination effect of bortezomib and trifluoperazine in U266 cells.

Bortezomib (nM)	Trifluoperazine (μ M)	Effect	CI	Conclusion
6.25	6.25	0.35	1.01	Additive
12.5	12.5	0.52	1.13	Antagonism
25	25	0.86	0.65	Synergism
50	50	0.91	0.95	Additive
100	100	0.93	1.61	Antagonism

Combination Index (CI) was calculated via CompuSyn software.

Table 2. Assessment of combination effect of bortezomib and trifluoperazine in MM.1S cells.

Bortezomib (nM)	Trifluoperazine (μ M)	Effect	CI	Conclusion
3.75	5	0.29	1.11	Antagonism
7.5	10	0.46	1.13	Antagonism
15	20	0.76	0.70	Synergism
30	40	0.84	0.88	Synergism
60	80	0.83	1.91	Antagonism

Combination Index (CI) was calculated via CompuSyn software.

slight change but no significant difference between experimental and control groups. The mean tumor weight of the control group was 1.30 g, the mean weight of the BTZ group and the TFP group was 0.45 g and 0.60 g, respectively, and the mean weight was 0.17 g in the combination group. We calculated the tumor suppression rate, the tumor suppression rate of the combination group was 87.18%, and the tumor suppression rate of the BTZ and TFP groups was 65.38% and 53.85%, separately. After that, we detected the expression of related proteins via IHC and western blot (Fig. 4). The expression of Ki-67 and Bcl-2 was decreased, and that of Bax, P53, Cleaved-Caspase 3 and Cleaved-Caspase 9 was increased. Compared with the BTZ group, the combination group was more significant ($p < 0.05$). These results suggested that TFP combined with BTZ exerts an anti-MM effect, and TFP could enhance the anti-MM effect of BTZ *in vivo*. Besides, we found no significant histopathological changes between the control and experimental groups (Fig. 5), which indicated that monotherapy and combination therapy could effectively inhibit tumor growth and have little toxicity on mice.

TFP might induce MM apoptosis by inhibiting p-P38 MAPK and NUPR1

Based on the above research, we noticed that TFP could play an anti-MM effect *in vivo* and *in vitro*. To explore the mechanism of TFP inducing apoptosis in MM, we found that the expression of p-P38 MAPK and NUPR1 was decreased after TFP treatment (Fig. 6A, B). Next, we used Anisomycin, a P38 MAPK agonist, to pretreat the MM cells; we found that Anisomycin could effectively reverse the apoptosis induced by TFP. Meanwhile, Anisomycin

also could reverse the decreased expression of NUPR1 induced by TFP (Fig. 6C, D). These results indicated that TFP might induce MM apoptosis by inhibiting p-P38 MAPK/NUPR1.

Discussion

Multiple myeloma is a common hematological malignancy, of which incidence is increasing. BTZ is the first proteasome inhibitor authorized by FDA for MM therapy and is widely used (Kouroukis et al. 2014; Mohty et al. 2014). BTZ can inhibit NF- κ B degradation to increase chemotherapy sensitivity, increase the expression of pro-apoptotic factor NOXA in tumor cells, up-regulate P21 and P27 cell cycle-dependent kinase inhibitor proteins, and inhibit angiogenesis (Lashinger et al. 2005; Cvek and Dvorak 2011; Piperdi et al. 2011). However, many patients develop resistance after BTZ treatment, which makes a poor prognosis. It is urgent to overcome the chemoresistance of BTZ.

TFP is a phenothiazine derivative and dopamine antagonist. It has antipsychotic and antiemetic activity and has been used clinically for more than 50 years. In recent years, researchers found that TFP has an anti-tumor effect in many cancers. TFP exerts anti-cancer effects by activating the Elk-1 and regulating the Ras/MEK/ERK pathway in human fibrosarcoma HT1080 cells (Shin et al. 2001). Researchers found that trifluoperazine can effectively reduce the chemoresistance of cisplatin-resistant urothelial cancer cells (Kuo et al. 2019). According to reports, TFP can effectively induce tumor suppression (Jiang et al. 2017; Feng et al. 2018; Qian et al. 2019). In our previous research, we discovered that TFP could induce multiple

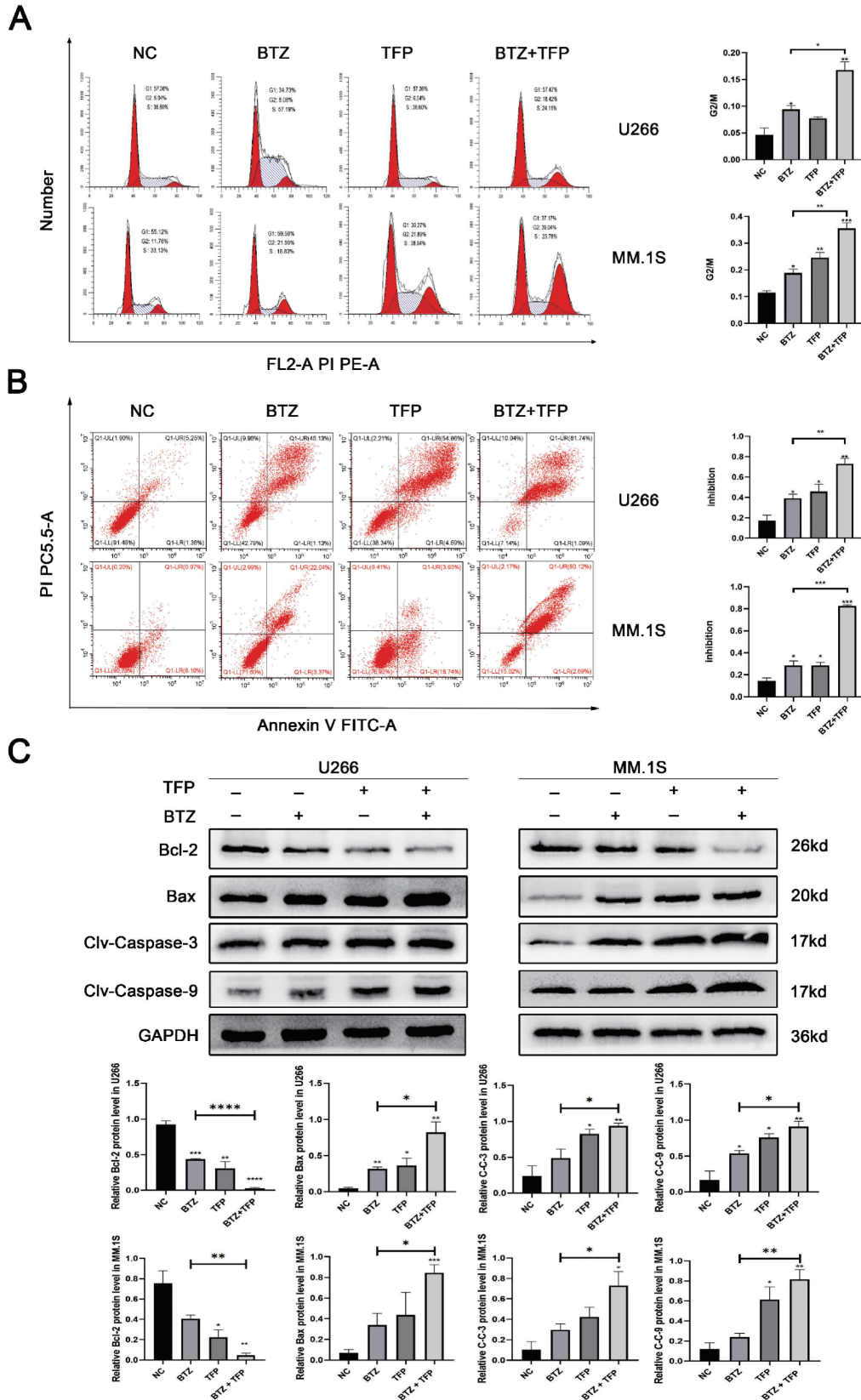


Fig. 2. Trifluoperazine (TFP) enhanced Bortezomib (BTZ)-induced G2/M cell cycle arrest and apoptosis in multiple myeloma cells. Cell cycle distribution was detected via flow cytometry (A). The apoptosis rate was detected via flow cytometry (B). The expression of apoptosis-related proteins was detected by western blot (C). Data are shown as mean \pm SEM for three replicate determinations. * p < 0.05, ** p < 0.01, *** p < 0.001, **** p < 0.0001.

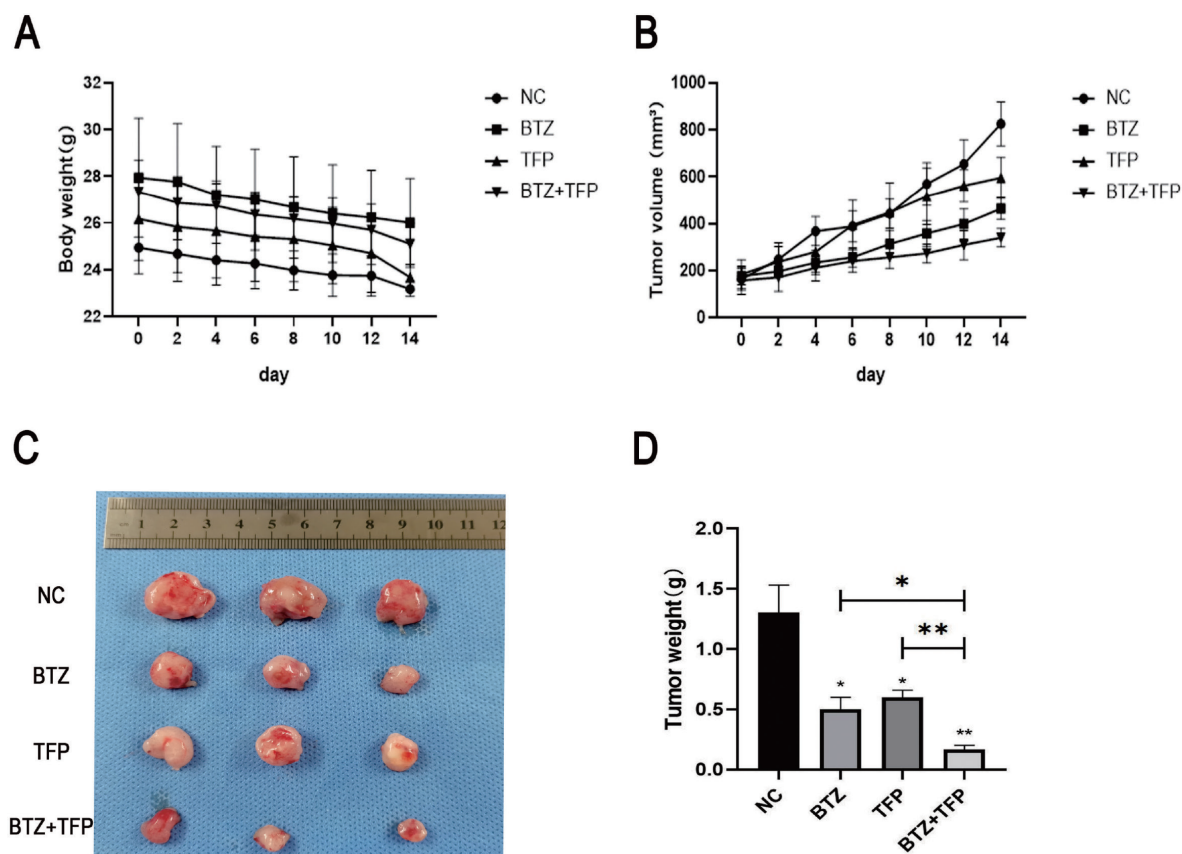


Fig. 3. Trifluoperazine (TFP) combined with Bortezomib (BTZ) exerts an anti-multiple myeloma effect *in vivo*. The weight of mice (A) and tumor volume (B) were recorded every two days during the experiment. After the administration, the tumors were excised, weighed (D), and photographed (C). Data are shown as mean \pm SEM. $n = 3$, $*p < 0.05$, $**p < 0.01$.

myeloma apoptosis by targeting NUPR1 *in vitro* (Li et al. 2020).

Combined strategies had been used to improve efficacy and reduce side effects for a long time; therefore, we want to explore whether BTZ combined with TFP could exert a better effect on inhibiting MM. This study concentrated on the combination of BTZ and TFP in multiple myeloma. It is the first time to illustrate the cooperation in BTZ and TFP causing MM apoptosis and inhibiting proliferation *in vivo* and *in vitro*. We found that TFP can synergistically lower the tumor burden in the MM.1S xenograft models, enhance BTZ-induced apoptosis and inhibit proliferation in U266 and MM.1S. Besides, we found that TFP could induce apoptosis in MM cells by inhibiting p-P38 MPAK/NUPR1.

The Cell Counting Kit-8 assay showed both BTZ and TFP could inhibit multiple myeloma cell viability via a dose-dependent manner. Our research discovered that BTZ combined with TFP could synergistically repress multiple myeloma cell viability *in vitro*. Cell cycle arrest benefits maintain gene stability. Some anticancer drugs exert effects by arresting the cell cycle (Nakayama and Nakayama 2006). Researchers have indicated TFP could induce G0/G1-phase cell cycle arrest in hepatocellular carcinoma and colorectal cancer cells (Jiang et al. 2017; Qian et al. 2019),

and another study showed that TFP could cause cell cycle arrest of L1210 leukemic lymphocytes at G2/M-phase (Sullivan et al. 2002). We discovered that TFP combined with BTZ could provoke G2/M-phase cell cycle arrest in U266 cells and MM.1S cells for the first time. We noticed that TFP could induce G2/M-phase cell cycle arrest in MM.1S while it could not induce G2/M-phase cell cycle arrest in U266. Therefore, further studies are required to clarify this issue.

Apoptosis is highly regulated cell death, also called cell suicide or programmed cell death (Belushkina and Severin 2001; Barisić et al. 2003). Our results indicated that both BTZ and TFP could induce U266 and MM.1S cells apoptosis and the combination group presented a more significant apoptosis rate than the single-agent group. To investigate the effect of BTZ and TFP used individually or in combination on multiple myeloma *in vivo*, we constructed the MM.1S xenograft models. After treatment with BTZ and TFP alone or in combination, we detected the apoptosis-related protein expression in tumor tissues by western blot. The results were consistent with the experiment *in vitro*. Ki-67 is a proliferation cell-related antigen whose function is closely associated with mitosis and is essential for cell proliferation (Sun and Kaufman 2018).

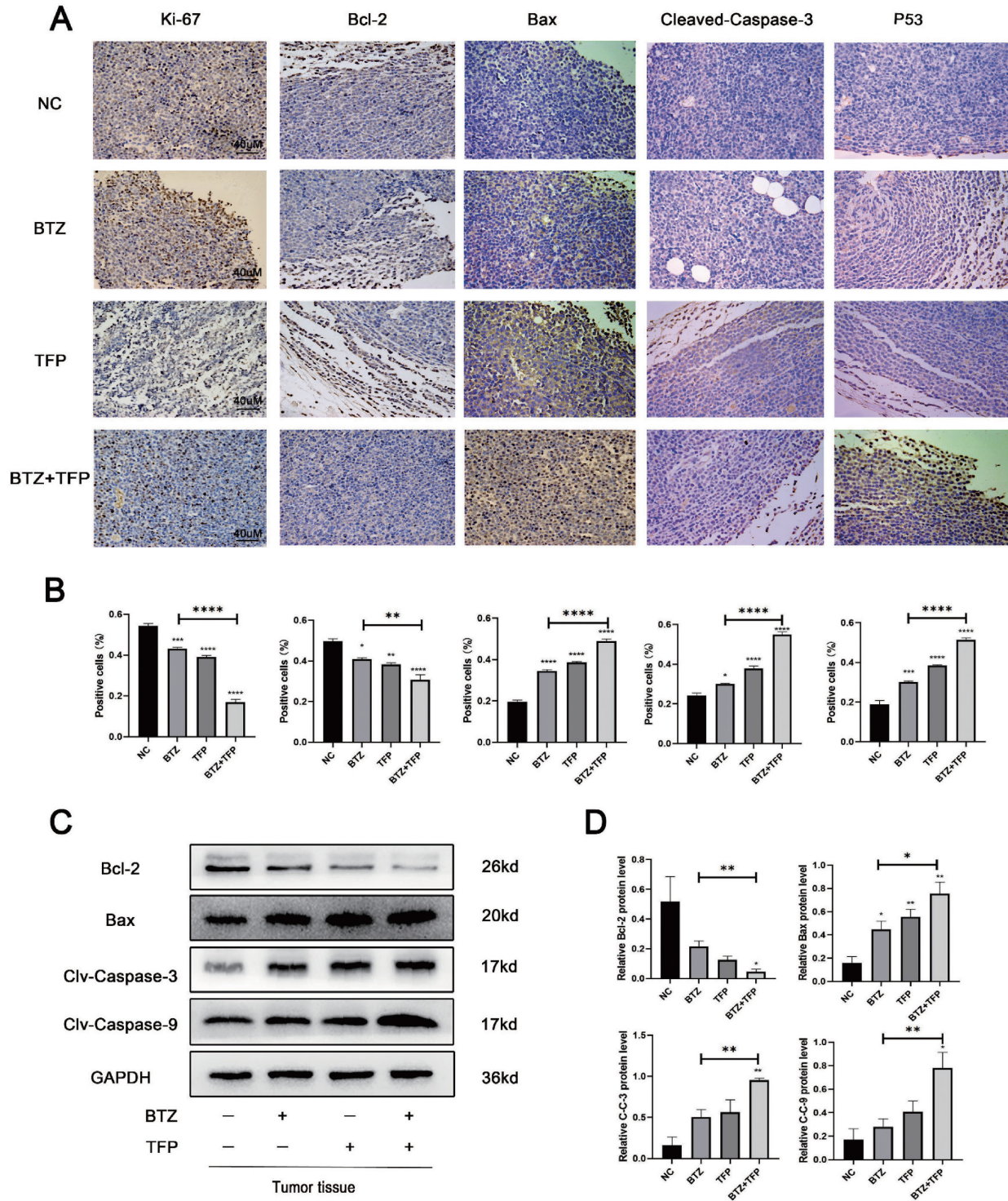


Fig. 4. The expression of apoptosis-related proteins in tumor tissues. Photographs of immunohistochemistry of Ki-67, Bcl-2, Bax, Cleaved-Caspase 3, and P53 in different groups (A). Magnification, × 400. The percentages of positive cells are shown (B). Western blot was used to detect the apoptosis-related proteins in tumor tissues (C and D). Data are shown as mean ± SEM. * $p < 0.05$, ** $p < 0.01$, *** $p < 0.001$, **** $p < 0.0001$.

P53 is a transcription factor and tumor suppressor protein that can regulate cell division, prevent DNA damaged or mutations cells from dividing, and transmit apoptosis signals to these cells through transcriptional regulation,

thereby preventing tumor formation (Levine et al. 1991). According to the IHC and HE staining, we noticed that the combination therapy could increase P53, decrease Ki-67, and have little toxicity *in vivo*. These results indicated that

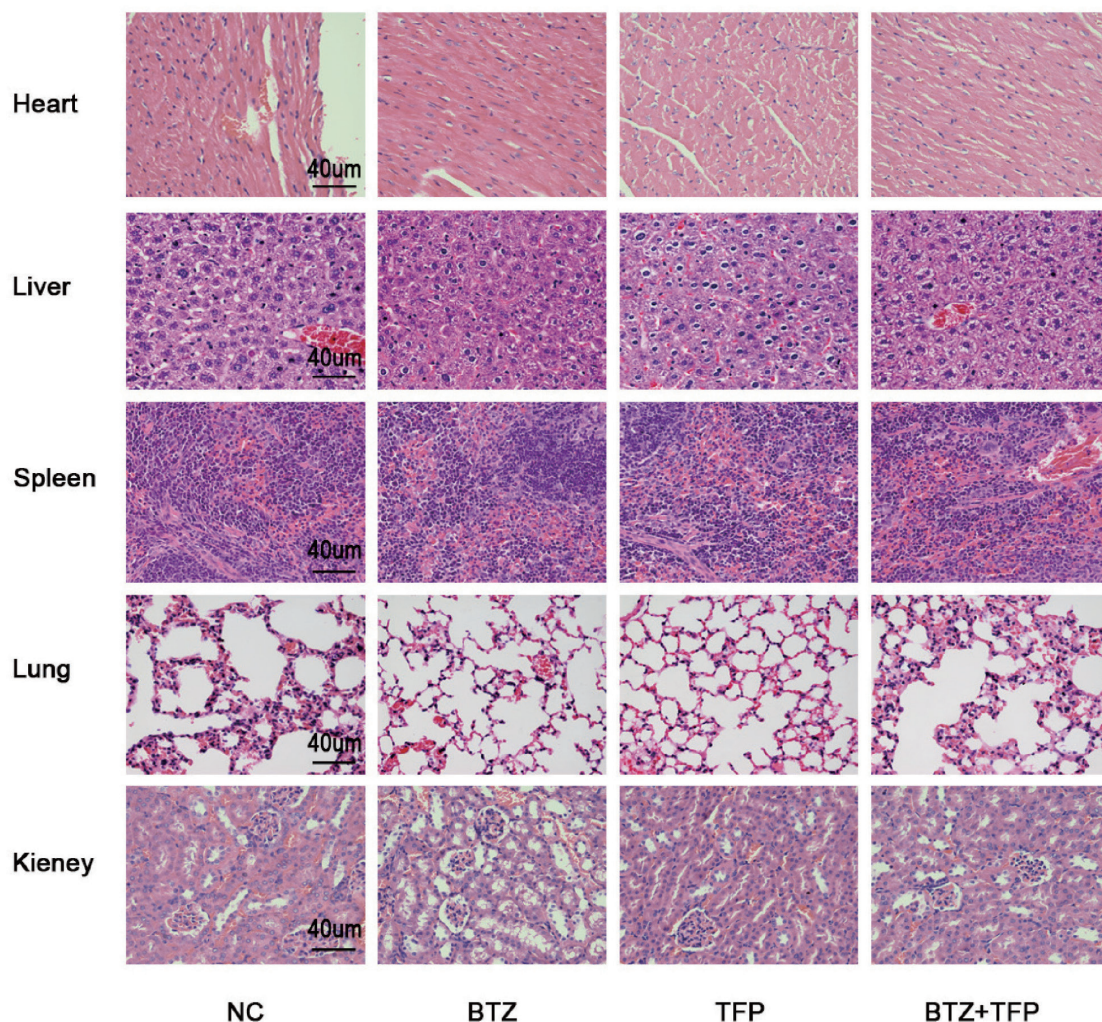


Fig. 5. Histopathological detection of major organs in MM.1S xenograft model. The major organ tissue was stained with hematoxylin-eosin and observed via a microscope: magnification, $\times 400$.

TFP might be an ideal drug for combination therapy with BTZ.

P38 MAPK is a member of the MAPK pathway and plays a vital role in cell apoptosis, inflammation, and chemoresistance. P38 MAPK is cell-specific and plays different roles in different cells. Shen Yue found that corilagin induces an anti-proliferation effect in rheumatoid arthritis by inhibiting P38 MAPK (Shen et al. 2021), and shikonin induces murine mammary cancer apoptosis via activating P38 MAPK (Xu et al. 2019). Increased P38 MAPK can induce chemoresistance in gastric cancer cells via affecting the Multidrug Resistance I gene (Guo et al. 2008). BTZ can increase the p-P38 MAPK expression in multiple myeloma and glioblastoma (Hideshima et al. 2004; Su et al. 2021). The BTZ-caused chemoresistance might be closely related to the activating of P38 MAPK in multiple myeloma. NUPR1 is a transcription regulator that regulates many processes such as cell cycle, apoptosis, autophagy, and DNA repair responses. It is highly expressed and maintains redox and antioxidant systems under various patho-

logical conditions, conferring chemotherapeutic resistance in cancer cells (Huang et al. 2021). Researchers found that P38 MAPK can induce NUPR1 expression in astrocytes and pancreatic cancer cells (Malicet et al. 2003; Carracedo et al. 2006). Previous studies suggested that TFP can bind to NUPR1 and induce cancer cells apoptosis (Santofimia-Castano et al. 2019). Our study found that TFP could reduce p-P38 MAPK and NUPR1, and P38 MAPK agonist could reverse the apoptosis and the decreased NUPR1 induced by TFP. Based on these results, we propose that TFP might induce MM apoptosis via inhibiting p-P38 MAPK/NUPR1, and it might be capable of overcoming the chemoresistance in MM (Fig. 7).

In summary, we observed that TFP could synergistically potentiate BTZ-induced anti-cancer effect on MM *in vivo* and *in vitro*. Our study suggests that TFP combined with BTZ may perform as a promising therapeutic strategy for multiple myeloma treatment.

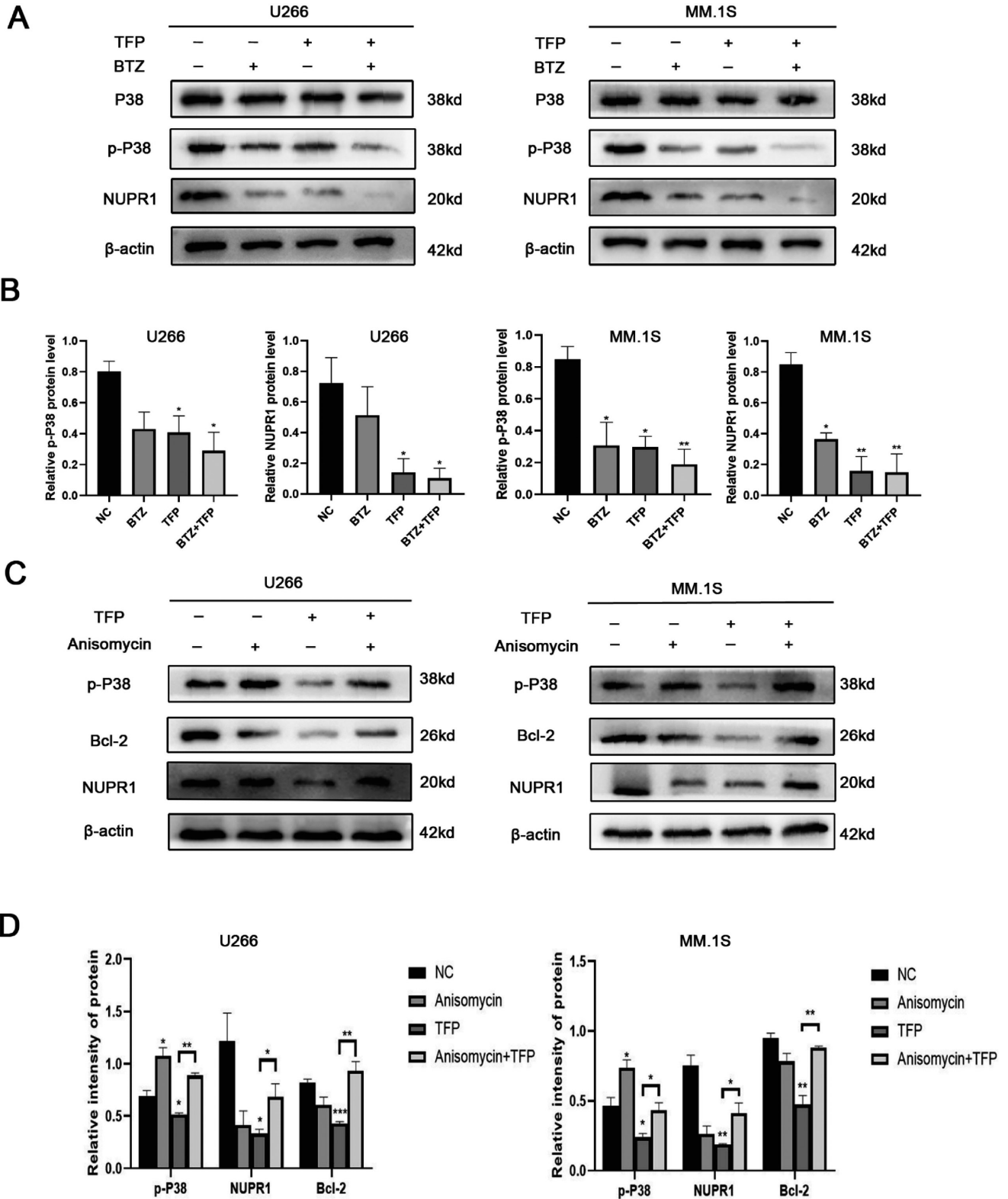


Fig. 6. Trifluoperazine (TFP) induced multiple myeloma apoptosis by inhibiting p-P38 MAPK/NUPR1. TFP, TFP combined with BTZ decreased the expression of p-P38 MAPK and NUPR1 in U266 and MM.1S (A and B). Anisomycin reversed the apoptosis and the decreased NUPR1 induced by TFP (C and D). Data are shown as mean ± SEM. * $p < 0.05$, ** $p < 0.01$, *** $p < 0.001$.

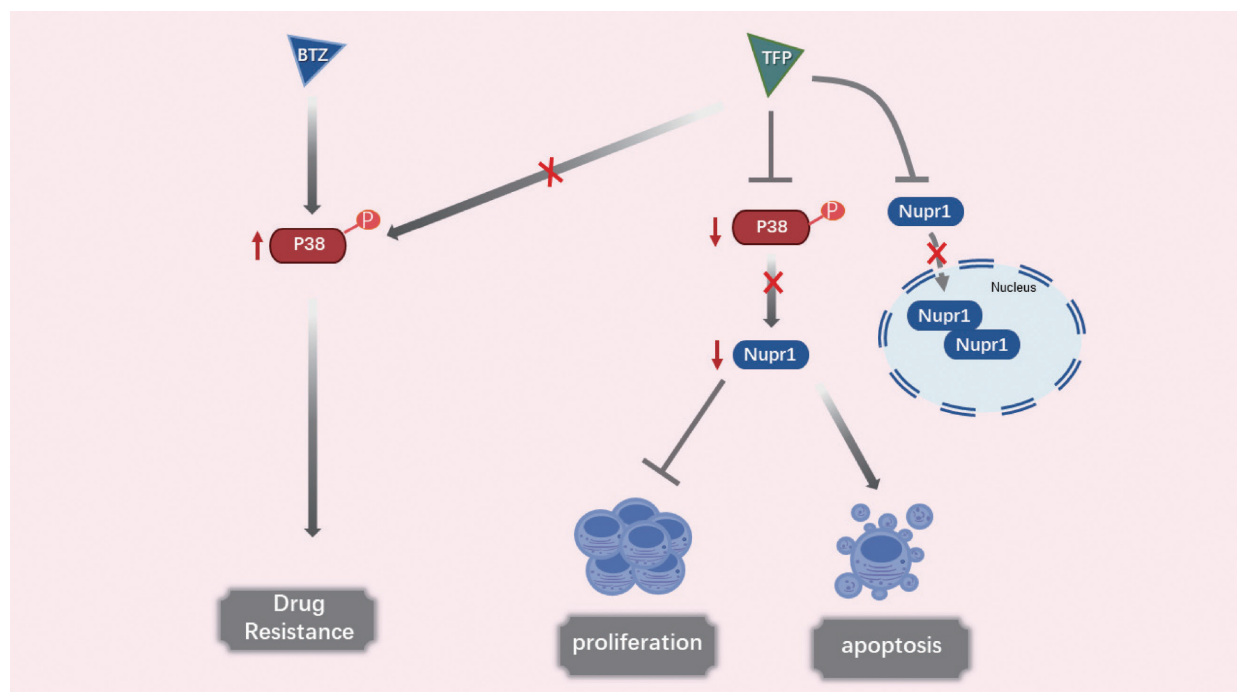


Fig. 7. The possible mechanism of Trifluoperazine (TFP) which induces apoptosis and reduces chemoresistance in multiple myeloma cells.

Acknowledgments

This work was supported by the Joint Medical Science Research Project of Chongqing (grant number 2021MSXM219) and the Chongqing Science and Technology Bureau (grant number cstc2019jcsx-msxmX0001). The authors are grateful for the support from the Experimental Research Central of the First Affiliated Hospital of Chongqing Medical University.

Conflict of Interest

The authors declare no conflict of interest.

References

- Ackler, S., Mitten, M., Foster, K., Oleksijew, A., Refici, M., Tahir, S., Xiao, Y., Tse, C., Frost, D., Fesik, S., Rosenberg, S., Elmore, S. & Shoemaker, A. (2010) The Bcl-2 inhibitor ABT-263 enhances the response of multiple chemotherapeutic regimens in hematologic tumors in vivo. *Cancer Chemother. Pharmacol.*, **66**, 869-880.
- Argyriou, A., Iconomou, G. & Kalofonos, H. (2008) Bortezomib-induced peripheral neuropathy in multiple myeloma: a comprehensive review of the literature. *Blood*, **112**, 1593-1599.
- Barisić, K., Petrik, J. & Rumora, L. (2003) Biochemistry of apoptotic cell death. *Acta Pharm.*, **53**, 151-164.
- Belushkina, N. & Severin, S. (2001) Molecular mechanisms of apoptosis pathology. *Arkh. Patol.*, **63**, 51-60.
- Carracedo, A., Egia, A., Guzman, M. & Velasco, G. (2006) p8 Upregulation sensitizes astrocytes to oxidative stress. *FEBS Lett.*, **580**, 1571-1575.
- Chen, R., Zhang, H., Liu, P., Wu, X. & Chen, B. (2017) Gambogic acid synergistically potentiates bortezomib-induced apoptosis in multiple myeloma. *J. Cancer*, **8**, 839-851.
- Chen, X., Luo, X. & Cheng, Y. (2018) Trifluoperazine prevents FOXO1 nuclear excretion and reverses doxorubicin-resistance in the SHG44/DOX drug-resistant glioma cell line. *Int. J. Mol. Med.*, **42**, 3300-3308.
- Cvek, B. & Dvorak, Z. (2011) The ubiquitin-proteasome system (UPS) and the mechanism of action of bortezomib. *Curr. Pharm. Des.*, **17**, 1483-1499.
- Feng, Z., Xia, Y., Gao, T., Xu, F., Lei, Q., Peng, C., Yang, Y., Xue, Q., Hu, X., Wang, Q., Wang, R., Ran, Z., Zeng, Z., Yang, N., Xie, Z., et al. (2018) The antipsychotic agent trifluoperazine hydrochloride suppresses triple-negative breast cancer tumor growth and brain metastasis by inducing G0/G1 arrest and apoptosis. *Cell Death Dis.*, **9**, 1006.
- Galmarini, D., Galmarini, C. & Galmarini, F. (2012) Cancer chemotherapy: a critical analysis of its 60 years of history. *Crit. Rev. Oncol. Hematol.*, **84**, 181-199.
- Guo, X., Ma, N., Wang, J., Song, J., Bu, X., Cheng, Y., Sun, K., Xiong, H., Jiang, G., Zhang, B., Wu, M. & Wei, L. (2008) Increased p38-MAPK is responsible for chemotherapy resistance in human gastric cancer cells. *BMC Cancer*, **8**, 375.
- Hideshima, T., Podar, K., Chauhan, D., Ishitsuka, K., Mitsiades, C., Tai, Y.T., Hamasaki, M., Raje, N., Hideshima, H., Schreiner, G., Nguyen, A.N., Navas, T., Munshi, N.C., Richardson, P.G., Higgins, L.S., et al. (2004) p38 MAPK inhibition enhances PS-341 (bortezomib)-induced cytotoxicity against multiple myeloma cells. *Oncogene*, **23**, 8766-8776.
- Huang, C., Lan, W., Fraunhofer, N., Meilerman, A., Iovanna, J. & Santofimia-Castaño, P. (2019) Dissecting the anticancer mechanism of trifluoperazine on pancreatic ductal adenocarcinoma. *Cancers (Basel)*, **11**, 1869.
- Huang, C., Santofimia-Castaño, P. & Iovanna, J. (2021) NUPR1: a critical regulator of the antioxidant system. *Cancers (Basel)*, **13**, 3670.
- Jiang, J., Huang, Z., Chen, X., Luo, R., Cai, H., Wang, H., Zhang, H., Sun, T. & Zhang, Y. (2017) Trifluoperazine activates FOXO1-related signals to inhibit tumor growth in hepatocellular carcinoma. *DNA Cell Biol.*, **36**, 813-821.
- Kang, S., Hong, J., Lee, J., Moon, H., Jeon, B., Choi, J., Yoon, N.,

- Paek, S., Roh, E., Lee, C. & Kang, S. (2017) Trifluoperazine, a well-known antipsychotic, inhibits glioblastoma invasion by binding to calmodulin and disinhibiting calcium release channel IP3R. *Mol. Cancer Ther.*, **16**, 217-227.
- Kouroukis, T., Baldassarre, F., Haynes, A., Imrie, K., Reece, D. & Chung, M. (2014) Bortezomib in multiple myeloma: systematic review and clinical considerations. *Curr. Oncol.*, **21**, e573-603.
- Kumar, S., Lee, J., Lahuerta, J., Morgan, G., Richardson, P., Crowley, J., Haessler, J., Feather, J., Hoering, A., Moreau, P., LeLeu, X., Hulin, C., Klein, S., Sonneveld, P., Siegel, D., et al. (2012) Risk of progression and survival in multiple myeloma relapsing after therapy with IMiDs and bortezomib: a multi-center international myeloma working group study. *Leukemia*, **26**, 149-157.
- Kuo, K., Liu, S., Lin, W., Hsu, F., Chow, P., Chang, Y., Yang, S., Shi, C., Hsu, C., Liao, S., Chang, H. & Huang, K. (2019) Trifluoperazine, an antipsychotic drug, effectively reduces drug resistance in cisplatin-resistant urothelial carcinoma cells via suppressing Bcl-xL: an in vitro and in vivo study. *Int. J. Mol. Sci.*, **20**, 3218.
- Lashinger, L., Zhu, K., Williams, S., Shrader, M., Dinney, C. & McConkey, D. (2005) Bortezomib abolishes tumor necrosis factor-related apoptosis-inducing ligand resistance via a p21-dependent mechanism in human bladder and prostate cancer cells. *Cancer Res.*, **65**, 4902-4908.
- Levine, A., Momand, J. & Finlay, C. (1991) The p53 tumour suppressor gene. *Nature*, **351**, 453-456.
- Li, A., Chen, X., Jing, Z. & Chen, J. (2020) Trifluoperazine induces cellular apoptosis by inhibiting autophagy and targeting NUPR1 in multiple myeloma. *FEBS Open Bio.*, **10**, 2097-2106.
- Malicet, C., Lesavre, N., Vasseur, S. & Iovanna, J. (2003) p8 inhibits the growth of human pancreatic cancer cells and its expression is induced through pathways involved in growth inhibition and repressed by factors promoting cell growth. *Mol. Cancer*, **2**, 37.
- Mateos, M. & San Miguel, J. (2017) Management of multiple myeloma in the newly diagnosed patient. *Hematology Am. Soc. Hematol. Educ. Program*, **2017**, 498-507.
- Mohty, M., Malard, F., Mohty, B., Savani, B., Moreau, P. & Terpos, E. (2014) The effects of bortezomib on bone disease in patients with multiple myeloma. *Cancer*, **120**, 618-623.
- Nakayama, K. & Nakayama, K. (2006) Ubiquitin ligases: cell-cycle control and cancer. *Nat. Rev. Cancer*, **6**, 369-381.
- Palumbo, A. & Cavallo, F. (2012) Have drug combinations supplanted stem cell transplantation in myeloma? *Hematology Am. Soc. Hematol. Educ. Program*, **2012**, 335-341.
- Piperdi, B., Ling, Y., Liebes, L., Muggia, F. & Perez-Soler, R. (2011) Bortezomib: understanding the mechanism of action. *Mol. Cancer Ther.*, **10**, 2029-2030.
- Qian, K., Sun, L., Zhou, G., Ge, H., Meng, Y., Li, J., Li, X. & Fang, X. (2019) Trifluoperazine as an alternative strategy for the inhibition of tumor growth of colorectal cancer. *J. Cell. Biochem.*, **120**, 15756-15765.
- Richardson, P., Weller, E., Lonial, S., Jakubowiak, A., Jagannath, S., Raje, N., Avigan, D., Xie, W., Ghobrial, I., Schlossman, R., Mazumder, A., Munshi, N., Vesole, D., Joyce, R., Kaufman, J., et al. (2010) Lenalidomide, bortezomib, and dexamethasone combination therapy in patients with newly diagnosed multiple myeloma. *Blood*, **116**, 679-686.
- Robak, P., Drozd, I., Szemraj, J. & Robak, T. (2018) Drug resistance in multiple myeloma. *Cancer Treat. Rev.*, **70**, 199-208.
- San Miguel, J., Schlag, R., Khuageva, N., Dimopoulos, M., Shpilberg, O., Kropff, M., Spicka, I., Petrucci, M., Palumbo, A., Samoilova, O., Dmoszynska, A., Abdulkadyrov, K., Schots, R., Jiang, B., Mateos, M., et al. (2008) Bortezomib plus melphalan and prednisone for initial treatment of multiple myeloma. *New Engl. J. Med.*, **359**, 906-917.
- Santofimia-Castano, P., Xia, Y., Lan, W., Zhou, Z., Huang, C., Peng, L., Soubeyran, P., Velazquez-Campoy, A., Abian, O., Rizzuti, B., Neira, J.L. & Iovanna, J. (2019) Ligand-based design identifies a potent NUPR1 inhibitor exerting anticancer activity via necroptosis. *J. Clin. Invest.*, **129**, 2500-2513.
- Shen, Y., Teng, L., Qu, Y., Liu, J., Zhu, X., Chen, S., Yang, L., Huang, Y., Song, Q. & Fu, Q. (2021) Anti-proliferation and anti-inflammation effects of corilagin in rheumatoid arthritis by downregulating NF- κ B and MAPK signaling pathways. *J. Ethnopharmacol.*, **284**, 114791.
- Shin, S., Kim, S., Kim, J., Min, D., Ko, J., Kang, U., Kim, Y., Kwon, T., Han, M., Kim, Y. & Lee, Y. (2001) Induction of early growth response-1 gene expression by calmodulin antagonist trifluoperazine through the activation of Elk-1 in human fibrosarcoma HT1080 cells. *J. Biol. Chem.*, **276**, 7797-7805.
- Su, Z., Han, S., Jin, Q., Zhou, N., Lu, J., Shangguan, F., Yu, S., Liu, Y., Wang, L., Lu, J., Li, Q., Cai, L., Wang, C., Tian, X., Chen, L., et al. (2021) Ciclopirox and bortezomib synergistically inhibits glioblastoma multiforme growth via simultaneously enhancing JNK/p38 MAPK and NF-kappaB signaling. *Cell Death Dis.*, **12**, 251.
- Sullivan, G., Garcia-Welch, A., White, E., Lutzker, S. & Hait, W. (2002) Augmentation of apoptosis by the combination of bleomycin with trifluoperazine in the presence of mutant p53. *J. Exp. Ther. Oncol.*, **2**, 19-26.
- Sun, X. & Kaufman, P. (2018) Ki-67: more than a proliferation marker. *Chromosoma*, **127**, 175-186.
- Turner, J., Dawson, J., Emmons, M., Cubitt, C., Kauffman, M., Shacham, S., Hazlehurst, L. & Sullivan, D. (2013) CRM1 inhibition sensitizes drug resistant human myeloma cells to topoisomerase II and proteasome inhibitors both in vitro and ex vivo. *J. Cancer*, **4**, 614-625.
- Xu, J., Koizumi, K., Liu, M., Mizuno, Y., Suzuki, M., Iitsuka, H., Inujima, A., Fujimoto, M., Shibahara, N. & Shimada, Y. (2019) Shikonin induces an antitumor effect on murine mammary cancer via p38dependent apoptosis. *Oncol. Rep.*, **41**, 2020-2026.